Published in final edited form as:
J Biomed Mater Res A. 2010 February ; 92(2): 451–462. doi:10.1002/jbm.a.32371.

In vivo bone biocompatibility and degradation of porous fumarate-based polymer/alumoxane nanocomposites for bone tissue engineering

Amit S. Mistry[1], **Quynh P. Pham**[1], **Corinne Schouten**[2], **Tiffany Yeh**[1], **Elizabeth M. Christenson**[1], **Antonios G. Mikos**[1], and **John A. Jansen**[2,*]

[1]Department of Bioengineering, Rice University, P.O. Box 1892, MS 142, Houston, Texas 77251-1892, USA [2]Department of Periodontology and Biomaterials, Radboud University Nijmegen Medical Center, P.O. Box 9101, 6500 HB Nijmegen, The Netherlands

Abstract

The objective of this study was to determine how the incorporation of surface-modified alumoxane nanoparticles into a biodegradable fumarate-based polymer affects *in vivo* bone biocompatibility (characterized by direct bone contact and bone ingrowth) and *in vivo* degradability. Porous scaffolds were fabricated from four materials: poly(propylene fumarate)/propylene fumarate-diacrylate (PPF/PF-DA) polymer alone; a macrocomposite consisting of PPF/PF-DA polymer with boehmite microparticles; a nanocomposite composed of PPF/PF-DA polymer and mechanically-reinforcing surface-modified alumoxane nanoparticles; and a low molecular weight PPF polymer alone (tested as a degradation control). Scaffolds were implanted in the lateral femoral condyle of adult goats for 12 weeks and evaluated by micro-computed tomography and histological analysis. For all material groups, small amounts of bone, some soft tissue, and a few inflammatory elements were observed within the pores of scaffolds, though many pores remained empty or filled with fluid only. Direct contact between scaffolds and surrounding bone tissue was also observed in all scaffold types, though less commonly. Minimal *in vivo* degradation occurred during the 12 weeks of implantation in all materials. These results demonstrate that the incorporation of alumoxane nanoparticles into porous PPF/PF-DA scaffolds does not significantly alter *in vivo* bone biocompatibility or degradation.

Keywords

Bone tissue engineering; Nanocomposite; Biocompatibility; Nanobiomaterials; Micro-computed tomography

INTRODUCTION

Bone tissue engineering strategies aim to regenerate natural bone tissue at the site of a severe bone defect by using a biomaterial scaffold to deliver the appropriate cells and/or growth factors to the defect. This scaffold must provide the appropriate mechanical properties, degradability, and bone biocompatibility to be effective. Mechanical properties

*Corresponding author: Dr. John A. Jansen, Professor and Chairman, Department of Periodontology and Biomaterials, Radboud University Nijmegen Medical Center, P.O. Box 9101, 6500 HB Nijmegen, The Netherlands, Tel: +31 (24) 3614920, Fax: +31 (24) 3614657, E-mail: J.Jansen@dent.umcn.nl.

No benefit of any kind will be received either directly or indirectly by the authors.

should be such that the scaffold will provide temporary support and stability to an injury site. Controlled degradation is another requirement since this creates space for developing tissue and facilitates gradual transfer of load to developing tissue. Bone biocompatibility refers to the ability of a material to support bone cell growth and function without eliciting a severe or harmful inflammatory response.1

Poly(propylene fumarate)/propylene fumarate-diacrylate (PPF/PF-DA) is a promising polymer for bone tissue engineering because its mechanical and degradation properties can be tailored for specific applications.2¯5 PPF-based materials have also been shown to be bone biocompatible in rats and rabbits.6,7 The mechanical properties of PPF/PF-DA can be further enhanced by the addition of a nano-sized ceramic component into the polymer matrix. Horch et al.8 discovered that the incorporation of surface-modified alumoxane nanoparticles into the PPF/PF-DA polymer network resulted in a three-fold gain in flexural modulus at very low loading concentrations. In a previous study, these PPF/PF-DA/alumoxane nanocomposites eroded, or lost mass, faster than the PPF/PF-DA polymer alone under accelerated degradation conditions.9 In the same study, the nanocomposite exhibited the same histocompatibility as the PPF/PF-DA polymer alone when implanted in the soft tissue of adult goats. Thus, the incorporation of alumoxane nanoparticles into the PPF/PF-DA polymer has been shown to enhance mechanical properties and degradation with no detrimental effect on the soft tissue response of the nanocomposite. When fabricated as a porous scaffold, these nanocomposites maintained their compressive mechanical properties for 12 weeks of *in vitro* degradation, albeit with minimal mass loss.10

In the current study, surface-modified alumoxane nanoparticles were again incorporated into the PPF/PF-DA polymer and formed into crosslinked, porous scaffolds. These scaffolds were implanted into the trabecular bone of adult goats for 12 weeks and evaluated by micro-computed tomography and histology. Through this work, we sought to answer the following question: How does the incorporation of surface-modified alumoxane nanoparticles into the PPF/PF-DA polymer affect: (1) *in vivo* bone biocompatibility, characterized by direct bone contact and ingrowth of bone into scaffold porosity; and (2) *in vivo* degradation?

MATERIALS AND METHODS

Porous, crosslinked fumarate-based scaffolds from three experimental groups and one control group were tested as described in Table 1: the PPF/PF-DA polymer alone; the macrocomposite (PPF/PF-DA polymer and micron-sized unmodified particles of boehmite —the mineral from which alumoxanes are synthesized); the nanocomposite (PPF/PF-DA polymer and surface-modified alumoxane nanoparticles); and the PPF degradation control (low molecular weight PPF polymer alone). Based on previous work by Horch et al.,8 the boehmite particles in the macrocomposite aggregate into large clusters that generally weaken a material. On the other hand, the surface-modified alumoxane nanoparticles in the nanocomposite provide mechanical reinforcement in flexion. Because of the relatively slow degradation of PPF/PF-DA-based materials, the PPF degradation control group, formulated to be less crosslinked and fast degrading, was included as a positive control for degradation.

Material Synthesis

Two batches of PPF (high and low molecular weight) were synthesized by established methods.10,11 The molecular weights of each polymer formulation were measured against polystyrene standards (Fluka, Buchs, Switzerland) by gel permeation chromatography (GPC) using a differential refractive index detector (Waters, Milford, MA) and a Styragel HR2 7.8 × 300 mm column (Waters). The PPF used in the PPF/PF-DA polymer, macrocomposite, and nanocomposite groups had a number average molecular weight of 2740 and a polydispersity index of 2.2. The low molecular weight formulation had a number

average molecular weight of 750 and a polydispersity index of 1.7. PF-DA was prepared according to methods described by Timmer et al.5 The identity of each polymer was verified by ^{1}H NMR (Bruker, Billerica, MA).

Research grade pseudo-boehmite particles were graciously provided by Sasol North America, Inc. (Houston, TX) and surface-modified alumoxane nanoparticles were synthesized from boehmite as described by Horch et al.8 Through these methods, alumoxane nanoparticles were modified first with a surfactant group to aid in the dispersion of the hydrophobic nanoparticles into the hydrophobic polymer. Then, a reactive acrylate group was added to the ends of the surfactant groups to enable the nanoparticle to participate in crosslinking. The functionalization of the resulting hybrid alumoxane nanoparticle was confirmed by Fourier transform infrared spectroscopy equipped with attenuated reflectance (FTIR-ATR) on a Nicolet 760 FT-IR (Thermo Nicolet, Waltham, MA).

Sample Fabrication

The formulation of each material group is described in Table 1. PPF and PF-DA polymers were combined in a 1:2 mass ratio in methylene chloride. Boehmite microparticles (1 wt.%) were added to form the macrocomposite group and hybrid alumoxane nanoparticles (1 wt. %) were added to the nanocomposite mixture. After several hours of mixing, methylene chloride was removed by rotary evaporation and vacuum drying. Low molecular weight PPF for the degradation control was used as prepared. A 0.1 g/ml solution of the photo-crosslinking initiator bis-(2,4,6-trimethylbenzoyl) phenylphosphine oxide (BAPO, Ciba Specialty Chemicals, Tarrytown, NY) was prepared in acetone and then added to the mixtures at 0.5 wt.%. Each group was then mixed with 80 wt.% of 300 – 500 μm NaCl salt crystals. After vigorous mixing, each blend was packed into cylindrical silicone rubber molds that were created with a fitted top and bottom. The molds were created using a master form of 4.5 mm diameter and 11.3 mm height such that the final sample would measure approximately 4 mm in diameter and 11 mm in height after crosslinking. Samples within the molds were photo-crosslinked in an Ultralum UV light box (Paramount, CA) under four bulbs that provided 365nm ultraviolet light at an intensity of approximately 3.5 mW/cm^2. After 5 min of crosslinking, samples were removed from the molds and treated for an additional thirty minutes in the light box. The polymer networks were then heat treated in a 60 °C oven for 12 hrs for additional crosslinking. Based on previous work with identical materials, unmodified boehmite particles aggregate into clusters several microns in diameter, while hybrid alumoxane nanoparticles remain in the nanophase, when mixed into the PPF/PF-DA polymer and crosslinked.8

Next, salt was leached from the scaffolds by immersion in water for three days at 37 °C on a shaker table (75 rpm) with water changed daily. After leaching, samples were rinsed in water, frozen, and lyophilized for 24 hrs. The mass of each scaffold was then measured and the percentage mass loss due to leaching (P_{ML}) was calculated by the following equation:

$$P_{ML} = \frac{m_F - m_L}{m_F} \times 100 \quad (1)$$

where m_F is the scaffold mass at fabrication and m_L is the scaffold mass after three days of salt leaching. Samples were press-fit into a steel mold of the defect size to make sure they were not too large for implantation. If a sample was too large to fit into the steel mold, it was lightly sanded to decrease its diameter. Finally, scaffolds were individually wrapped in gauze, placed in a histological cassette, and sterilized by exposure to ethylene oxide for 12 hours in a ventilated sterilizer (Andersen Products, Haw River, NC).

Animal Model

Adult Saane goats were chosen for this study because their healing and reaction to biomaterials is similar to that of humans.12 The nine adult goats used for this experiment were housed in a stable for the duration of this project except for the surgeries, which were performed in an animal hospital. Before surgery, blood samples of the animals were taken to ensure that the animals were free of Caprine Arthritis Encephalitis / Caseous lymphadenitis (CAE/CL). The Dutch national guidelines for the care and use of laboratory animals were observed throughout this study.

Implantation

Implantation surgery closely followed methods described by Bernhardt et al.13 Samples were implanted in holes drilled into the lateral side of one or both of the femoral condyles of the goats. Six goats received implants in either the right or left condyle while three goats received implants on both sides. Two samples from different material groups were installed per bone resulting in a total of two or four implants per animal.

The operation was performed under general anesthesia induced by an intravenous injection of pentobarbital and maintained with Isoflurane 2.4% through a constant volume ventilator which was administered through an endo-tracheal tube. To reduce the risk of peri-operative infection, the goats were treated with antibiotics as follows. During the operation, Albipen® (15%, 3 ml/50 kg) was administered subcutaneously. Albipen® LA (7.5 ml/50 kg) was again administered subcutaneously one day and three days after the operation. Goats also received Finadyne® for two days postoperatively to reduce pain.

To begin the surgery, the goat's hind limbs were shaved, washed, and disinfected with povidone iodine. A longitudinal incision was made on the lateral surface of the left or right femur. Then, the periosteum was reflected and one or two titanium bone markers were placed in the bone area. X-ray imaging was then used to localize the implant site in trabecular bone. A 2.0-mm pilot hole was drilled and gradually widened with drills of increasing size until the final diameter was 4 mm. This was achieved using a gentle surgical technique of low rotational drill speeds and continuous cooling with saline. Two holes were made in the lateral condyle (superior and inferior) with a distance of at least 0.5 cm between the holes. Samples were then carefully press-fit into the defects and each site was irrigated and packed with sterile cotton.

Six scaffolds were implanted from each material group ($n = 6$) such that all scaffolds in an implant site were from different groups. Each goat received two or four implants and the location of material groups was rotated in each animal. After the insertion of implants, the soft tissue was closed in separate layers using sutures. Postoperative x-rays were used to confirm implant placement and filling.

Histological Specimen Preparation

At the end of 12 weeks, animals were euthanized with an overdose of Nembutal®. Immediately afterwards, the femoral condyles were excised and excess tissue was removed. A diamond saw was used to cut the condyle into smaller pieces. Samples were fixed in a 10% buffered formalin solution and stored in ethanol. Then, samples were scanned by micro-computed tomography (micro-CT, details below). Next, samples were dehydrated in an ethanol series and embedded in methyl methacrylate.

A modified diamond blade sawing microtome was used to prepare non-decalcified sections of 10 – 15 μm thickness. Three sections were made in a sagittal direction perpendicular to the longitudinal axis of the implant. In addition, sections were made in three regions of the

implant: the top (surface), the middle, and the bottom (bone). Sections were stained using methylene blue and basic fuchsin during the sectioning process and examined using light microscopy.

Micro-Computed Tomography (Micro-CT)

Prior to sectioning, a Skyscan Desktop MicroCT 1172 (Aartselaar, Belgium) with a source voltage of 100 kV and a current of 100 μA was used to acquire X-ray radiographs of implants and surrounding tissue. The machine was equipped with a 1.0 mm Aluminum filter and set to a resolution of 17.1 μm. Bone samples were wrapped in parafilm and affixed to a rotating stage which acquired radiographs every 0.7° up to 180°. Due to the large variation in bone specimen size, cross-sectional slices were reconstructed with individualized thresholding values to accurately distinguish bone and air. For analysis, a cylindrical volume of interest (VOI) of 6.85 mm diameter and 5.00 mm height was created around the implant's mid-section. Bone volume was measured within this region and compared across material groups.

Histological Analysis

Sections were observed by light microscopy and independently scored by two blinded observers (ASM and QPP) according to the scales shown in Table 2. When the two observers disagreed on a score, the section was discussed until a consensus was reached. In most cases, three scores for each region (top, middle, or bottom) of a sample were averaged and then scores for all the samples in a group were averaged to give a score for each region of each material group.

Bone ingrowth within the pores of the scaffolds was evaluated based on the presence and quality of bone, fibrous tissue, and inflammatory elements throughout the pores of the scaffold based on established guidelines.[7,14] Bone contact at the bone-scaffold interface was scored based on the presence and quality of bone, fibrous tissue, and/or inflammatory elements between the outer edge of the implant and the surrounding bone tissue based on a scoring guide modified from Jansen et al.[15] The degradation of the scaffolds was also scored based on fragmentation and crack formation throughout scaffolds as described previously.[9,16] Additionally, if any amount of bone was observed within the pores of a scaffold in a section, a note was made and counted. A similar count was made for the occurrence of direct contact between a scaffold and the surrounding bone tissue.

Statistical Analysis

All data are presented as mean ± standard deviation for each experimental group. Mass and size measurements of scaffolds were made for nine scaffolds per group ($n = 9$). Percent mass loss due to salt leaching was measured for a sample size of 12 ($n = 12$). Six scaffolds per material group were implanted for the *in vivo* experiment. However, some samples could not be analyzed due to difficulties during implantation or retrieval. If a section contained a cut scaffold or a portion of cortical bone, marrow, or growth plate, it was excluded from analysis. Micro-CT analysis was conducted for $n = 5 – 6$ and histological scoring was completed for $n = 3 – 6$. The number of histological sections analyzed per region of each material group ranged from 7 to 21. Nevertheless, the sample size for each group was large enough to allow for statistical comparisons.

Single-factor analysis of variance (ANOVA) was used to determine statistical significance within data sets. If ANOVA detected a significant difference within a data set, Tukey's honestly significantly different (HSD) multiple comparison test was used to determine significant differences between material groups. All tests were conducted with 95% confidence intervals ($p < 0.05$).

RESULTS AND DISCUSSION

This study evaluated the effect of incorporating surface-modified alumoxane nanoparticles into the PPF/PF-DA polymer on: (1) *in vivo* bone biocompatibility, characterized by bone ingrowth and bone contact; and (2) the *in vivo* degradation of the scaffold.

Sample Fabrication

Porous scaffolds were fabricated by photo-crosslinking polymer/salt mixtures followed by leaching out of the salt. Scaffolds produced by this method were 4.0 ± 0.1 mm in diameter and 11.1 ± 0.2 in height with negligible differences between material groups. Likewise, there was no significant difference in the mass of PPF/PF-DA alone, macrocomposite, and nanocomposite scaffolds, which weighed 43.9 ± 2.2 mg. However, the PPF degradation control scaffolds weighed significantly more, 47.5 ± 1.4 mg.

All polymer networks lost more than 80% of their mass during salt leaching, indicating that all the salt was leached out leaving behind an interconnected porous network. The PPF/PF-DA alone, macrocomposite, and nanocomposite samples lost 81.7 ± 0.5 %, 81.7 ± 0.7 %, and 81.3 ± 0.6 % of their mass during leaching. Interestingly, the PPF degradation control group lost significantly more than the other groups, 84.0 ± 0.5 % ($p < 0.05$), suggesting that either unreacted components or degradation products were also leached during the three day leaching period. Based on previous work, PPF and PPF/PF-DA are known to degrade very slowly and that negligible degradation would have occurred during the three day leaching period.[3,17] Thus, the greater than expected mass loss during leaching, especially by the PPF degradation control group, was attributed to the removal of unreacted, water-soluble components.

Micro-Computed Tomography

Micro-CT has proven to be a very useful, non-destructive tool for tissue engineering studies. This technique provides a means to analyze the architecture of a tissue engineering scaffold before implantation[18] and also enables the measurement of bone volume and bone density in and around a bone defect.[19] PPF-based polymer scaffolds can be scanned alone by micro-CT, but the scanning of bone tissue requires the use of an aluminum filter that makes the polymeric implant within bone radiographically transparent. The incorporation of a 1 wt.% loading of boehmite or alumoxane particles into the polymer scaffolds was not large enough to noticeably affect their radiographic intensity. Thus, all implants appeared as blank space within the bone samples during scanning. Figure 1 depicts a representative cross-section of a bone sample.

To calculate bone volume in and around scaffolds, a VOI was defined around the mid-section of each implant with a diameter of 6.85 mm (larger than the implant diameter) and a height of 5.00 mm. Bone volume in this region was quantified using micro-CT reconstruction and analysis software. As shown in Table 3, no significant differences in bone volume were observed between the four material groups. Reconstructed models of samples from all groups showed little or no bone formation inside scaffolds (Figure 1). Based on these results, the addition of boehmite or alumoxane particles into the PPF-based polymer did not significantly affect bone growth into the porous structure of scaffolds.

One potential source of error in these measurements arose from the fact that the bone samples retrieved from goats were of varying size and shape. Therefore, each sample was reconstructed with its own unique thresholding parameters, which are used to distinguish air and bone. Comparisons between two samples that were assigned different thresholding values are less reliable. Furthermore, implants were not always placed into the femoral condyle parallel to each other. This factor, compounded with the difficulty of orienting

samples perpendicular to the micro-CT stage, also affected the error of this analysis. Nevertheless, qualitative observations of micro-CT reconstructions provided minimal evidence of bone growth within the implanted scaffolds. Some possible reasons for the lack of bone growth in the scaffolds may be: small pore sizes, low porosity, lack of pore interconnectivity, or poor bone biocompatibility of the materials. To further explore these possible explanations, histological tools were utilized as described in the following section.

Histological Analysis

After implantation for 12 weeks, scaffolds and their surrounding bone were retrieved, sectioned, and stained for histological observation and analysis. In these sections, polymer-based scaffolds were easily visualized as a white material, which did not absorb either stain, surrounded by blue- and red-stained tissue. The square-shaped pores, observed within the scaffolds, resulted from the leaching of cubic salt crystals. While these pores often appeared to be isolated from one another in two dimensions, micro-CT analysis in previous work demonstrated that the pores were interconnected in three dimensions.[10,11] The biological response towards the scaffolds varied greatly from sample to sample and from goat to goat. Generally, small amounts of immature bone, some soft tissue infiltration, a few markers of inflammation, and some evidence of *in vivo* degradation were observed in and around scaffolds, though many scaffold pores remained empty or filled with fluid only. Histological analysis of the bone ingrowth and bone contact of fumarate-based/alumoxane nanocomposites involved evaluation of the area within the pores of scaffolds and at the bone-scaffold interface. Histological methods were also used to assess the *in vivo* degradation of the scaffolds in terms of fragmentation.

Bone growth in scaffold pores—Bone formation within the pores of scaffolds, as shown in Figure 2, was observed in several sections. Generally, immature bone developed in pores towards the outer edges of scaffolds. However, bridging through a scaffold was not observed in any section and only small amounts of bone were deposited in sections where bone was observed. The occurrence of any amount of bone in scaffold pores was counted for each region and material group and is shown in Table 4. Almost all scaffolds analyzed (20 out of 21) had some quantity of bone tissue within their pores in at least one section. Out of 159 sections examined, immature bone was observed in 92 sections (58% of all sections). Bone growth in the PPF/PF-DA-based materials (PPF/PF-DA polymer alone, macrocomposite, and nanocomposite) was detected in 60 – 70% of the sections for each group, with occurrence most prevalent in the PPF/PF-DA polymer alone scaffolds. On the other hand, immature bone was observed in only 23% of the sections of the PPF degradation control group. The PPF degradation control group differed from the other groups in that it was composed of lower molecular weight PPF without the PF-DA crosslinker and also has been shown to possess lower mechanical properties and less pore interconnectivity than the PPF/PF-DA-based groups.[10] Any combination of these factors may have resulted in the lower occurrence of bone in the PPF control group.

Irrespective of the presence of bone, the pores of many scaffolds were infiltrated by soft tissue as shown in Figure 3. In most cases the tissue was organized as fibrous layers, but in some instances the infiltrated tissue was disorganized and contained inflammatory elements. The level of inflammatory response varied widely with some scaffolds containing only a few inflammatory elements (Figure 3) and others containing clusters of inflammatory cells including macrophages and occasional foreign body giant cells (Figure 2). Another common observation was the presence of empty or fluid-filled pores.

Qualitative scoring of bone ingrowth within pores is shown in Figure 4. Scores generally ranged from 1 to 2 with no significant differences between any material groups in any

region. A score of 1 corresponded to pores filled with mostly inflammatory elements and some connective soft tissue (with or without bone) or pores that remained empty or filled with fluid. A score of 2 signified pores filled mostly with soft tissue and some inflammatory elements. Higher scores indicated pores filled with more bone than soft tissue. While some quantity of bone was observed in more than 60% of the sections examined, only 3 scaffolds received a score of 3 and no scaffold received a score of 4. Thus, few scaffolds contained mostly bone and very few contained significant bone growth without inflammation. Based on qualitative scoring, the composition of material had no significant effect on bone growth in scaffold pores. However, bone formation in the pores of scaffolds was observed much more frequently in the PPF/PF-DA-based materials than in the PPF degradation control group.

The use of a ceramic nano-filler was expected to encourage bone formation and growth due to the favorable bone biocompatibility of ceramic materials and the increased surface area of nanoscale particles. For example, Webster et al.20 demonstrated that osteoblast cells cultured *in vitro* on nanophase ceramics experienced enhanced proliferation and osteoblast function compared to conventional (non-nanophase) materials. Lewandrowski et al.21 implanted PPF-based scaffolds with nanoscale and microscale hydroxyapatite (HA) into rat tibia defects and observed greater bone formation in the PPF/nano-HA compared to the PPF/micron-HA. It should be noted that Lewandrwoski et al. used a different formulation of the PPF polymer and a higher loading (~14 wt.%) of HA, which is a very bone-friendly substance. In our work, a very low loading concentration (1 wt.%) of alumoxane nanoparticles was applied to the polymer since that was previously shown to yield the maximum mechanical reinforcement of PPF/PF-DA.8 Thus, it appears that higher alumoxane concentrations are required to observe their effect on bone formation; however higher concentrations may also result in diminished mechanical properties.

The results of this histological analysis concur with the results of micro-CT analysis in that minimal bone formation was observed in the pores of the PPF/PF-DA alone, macrocomposite, and nanocomposite scaffolds. Instead of bone, many pores were filled with soft tissue, inflammatory elements, or simply remained empty. This may be a result of the compatibility with the material itself or the porous architecture of scaffolds. Small pore sizes, low porosity, or lack of pore interconnectivity may have influenced the pore architecture in a manner to reduce bone and soft tissue infiltration into the scaffold. In this study, the salt porogen used was sieved to retrieve salt particles 300 – 500 μm in size. This size was selected to produce pores in the scaffolds large enough to allow cell and tissue infiltration without compromising mechanical integrity. Previous *in vitro* work with biodegradable polymer scaffolds demonstrated that pore sizes from 150 μm to 710 μm support cell proliferation and osteogenic cell function.22،23 Fisher et al.6 varied pore size and porosity of salt-leached PPF-scaffolds and implanted them in rabbit cranial defects for 8 weeks and found that neither pore size nor porosity significantly affected tissue response or bone growth into the pores.

In regards to porosity, scaffolds were fabricated with 80 wt.% NaCl porogen to produce 70 vol.% scaffolds. It has been shown that lower porosities may not yield an interconnected network while higher porosities compromise mechanical properties.17،24 Another factor that influenced the pore architecture of scaffolds was pore interconnectivity. In this study, adequate pore interconnectivity within scaffolds was established based on complete leaching of salt. In a previous study, micro-CT methods were used to compute the pore interconnectivity of scaffolds.10 Porous scaffolds fabricated from the PPF/PF-DA polymer alone, the macrocomposite, and the nanocomposite were 97 – 99% interconnected when analyzed for connection sizes of at least 29 μm.10 However, all scaffolds became less interconnected when analyzed at larger pore connection sizes. Histological images from the

current study reveal that many pores appeared isolated in two-dimensions and some of these pores remained empty or were simply filled with fluid after 12 weeks *in vivo*. Thus, it appears that the interconnectivity of scaffold pores was adequate for complete salt leaching but may not have been sufficient for tissue infiltration and bone ingrowth throughout the scaffolds.

As an additional note about fabrication methods, silicone molds were used to produce porous, photo-crosslinked PPF-based scaffolds. One potential concern about this method is that packing polymer/salt mixtures into the molds may have resulted in lower pore connectivity on the exterior surface of samples. This was observed in the outer edges of some scaffolds (e.g., the far right area of Figure 2a), but was not very common.

Bone contact at interface—The occurrence of direct contact at the interface between scaffolds and surrounding bone tissue was used as another indicator of bone biocompatibility. Figure 5a is an example of direct bone contact between the implant and the surrounding polymer network. However, observations of direct bone contact were not common and were localized to only a few sparse areas on a scaffold. Indeed, no scaffold experienced a majority of direct contact with surrounding bone. The occurrence of direct bone contact, based on visual observation and counting, is presented in Table 5. Out of all the scored sections, 39% showed some level of direct bone contact and the PPF degradation control group demonstrated the highest occurrence (58%).

The presence of a thin fibrous capsule between an implant and surrounding bone tissue, as shown in Figure 5b, was the predominant observation. In some cases, the capsule formed adjacent to a pore, thus creating a pocket in which inflammatory cells would sometimes accumulate. Figure 5c shows a more pronounced response including disorganized and inflamed tissue and various inflammatory cells between bone and the scaffold. However, these responses were less frequent than the presence of fibrous capsules.

Qualitative scoring of bone contact at the bone-scaffold interface, based on the scoring guidelines established in Table 2, is presented in Figure 6. No scaffold demonstrated direct contact with a majority of the surrounding bone tissue (score of 4) and no scaffold was in contact with remodeling bone at the interface (score of 3). All material groups received an average score of about 2, which corresponded to the presence of a fibrous tissue capsule around the implant. Additionally, a small number of implants were surrounded by unorganized or inflamed tissue (score of 0 or 1). No significant differences were observed between any material groups or scaffold regions. Thus, the presence of boehmite microparticles or alumoxane nanoparticles in PPF/PF-DA did not have an effect on bone contact with the composite scaffolds.

Various studies have been conducted to evaluate the bone biocompatibility of fumarate-based materials. For example, Peter et al.25 demonstrated that fumarate-based polymer networks support osteoblast cell growth and function *in vitro*, though it should be noted that the polymer from this study was quite different from the polymers used in the current work. A few studies have also demonstrated the *in vivo* bone biocompatibility of PPF-based materials. For instance, minimal direct bone contact and bone ingrowth were observed when Fisher et al.6 implanted photo-crosslinked, porous PPF scaffolds in rabbit cranial defects. Interestingly, significant bone formation and favorable contact with bone have been observed when PPF-based materials were combined with growth factors.7,26 In these instances, however, it is likely that the osteoinductivity of the growth factor components overshadowed the bone biocompatibility of the polymer scaffolds. In the current study, the addition of a 1 wt.% loading of alumoxane nanoparticles into the PPF/PF-DA polymer was not sufficient to influence bone ingrowth and bone contact. A larger concentration of the

ceramic nanoparticle may have influenced these properties more, though this would have compromised the mechanical reinforcing properties of the nanoparticles.

Degradation—Observations of fragmentation, crack formation, and dissolution were used to indicate the degradation of polymeric scaffolds. The image in Figure 7 depicts extensive fragmentation around the upper left side of the scaffold accompanied by a great deal of fibrous soft tissue infiltration and very few inflammatory elements. These observations, which occurred primarily in the PPF degradation control group, indicate that *in vivo* degradation occurred during the 12 week study.

There was a great deal of variation in the qualitative scoring of the degradation of scaffolds, as shown in Figure 8. The extents of degradation observed in the PPF/PF-DA polymer alone, macrocomposite, and nanocomposite groups were not significantly different due to this large variation. In contrast, the PPF degradation control received a significantly higher degradation score for its top region in comparison to the top regions of the other materials. When the scores of all regions were combined, the PPF control also exhibited a significantly higher score than all other groups ($p < 0.05$). As expected, more *in vivo* degradation occurred among PPF control scaffolds that were formulated with lower molecular weight PPF and were less crosslinked than the PPF/PF-DA-based materials.

One potential cause for the relatively high variation in the degradation scoring is the possibility that fragmentation occurred by means other than degradation. The scaffolds were fabricated to fit precisely within the drilled holes to minimize motion after implantation. However, the act of press-fitting scaffolds into the defect sites may have resulted in some fragmentation at the time of implantation. It is possible that a score of 1 (corresponding to minor crack formation and fragmentation) might have been wrongly assigned to a scaffold that simply fragmented during implantation. To minimize this effect, degradation scores of 2 or higher were given only when scaffolds experienced very obvious fragmentation in various locations around the implant. Regardless of this correction, the PPF degradation control demonstrated significantly more degradation in its top region and overall compared to the other materials ($p < 0.05$). Various other studies of PPF-based materials have also demonstrated minimal *in vivo* degradation.[6,9,26] For instance, Hedberg et al.[14] studied the *in vivo* degradation of PPF/PF-DA scaffolds loaded with PLGA microparticles after 12 and 18 weeks in rabbit radii and observed minimal fragmentation and very few indications of degradation.

Previous work demonstrated that the PPF/PF-DA/alumoxane nanocomposites degrade faster than the PPF/PF-DA polymer alone networks when fabricated as solid discs and degraded under accelerated conditions.[9] Unfortunately, this effect was not observed in the current study when scaffolds were fabricated as porous scaffolds and implanted in adult goats. Once again, the loading concentration of nanoparticles may not have been high enough to influence degradation. Alternatively, the duration of the study may have been too short to observe a degradation effect.

An overall difficulty in this study was that histological observations varied widely from goat to goat, sample to sample, and scaffold region to scaffold region. For example, Figure 2 and Figure 3 are from two regions of the same scaffold, yet depict very different responses. Some variation within the results of animal studies is generally expected, and therefore, higher sample sizes are used to draw conclusions and make comparisons. In this work, some samples and regions of scaffolds were excluded from analysis due to implantation, processing, or sectioning problems. Nevertheless, the sample size for histological analyses, though lower than originally intended, was large enough to facilitate thorough statistical analyses.

Qualitative histological scoring is a well established method for the evaluation of bone ingrowth, bone contact, and degradation of bone tissue engineering scaffolds.15 Another option, histomorphometrical analysis, was not deemed useful since very small amounts of bone formation in scaffolds were observed. In a previous study, mass and volume loss, mechanical properties, and network analysis were used to characterize the *in vitro* degradation of the same materials.10 In the current study, these methods could not be employed because of the soft and hard tissue in and around implants after extraction.

Histological scoring guides are based on an ideal score of 4 and a worst-case scenario score of 0 or 1. Thus, even though many of the PPF-based materials evaluated in this study received low histological scores, they do merit further study for use in bone tissue engineering. These PPF-based materials were developed with the goal of enhancing mechanical properties while maintaining degradability. With this in consideration, PPF/PF-DA/alumoxane nanocomposites have the potential to be competent tissue engineering scaffolds with further efforts to improve their biological interactions.

CONCLUSIONS

The goal of this study was to determine the effect of incorpating surface-modified alumoxane nanoparticles into a biodegradable fumarate-based polymer on *in vivo* bone biocompatibility and degradability. Porous scaffolds fabricated from the PPF/PF-DA polymer, the PPF/PF-DA/boehmite macrocomposite, the PPF/PF-DA/alumoxane nanocomposite, and a PPF degradation control were implanted in the trabecular bone of adult goats and evaluated. Based on micro-CT and histological analysis, small quantities of bone, limited direct contact, and minimal degradation were observed after 12 weeks of implantation. Nevertheless, the loading of 1 wt.% of alumoxane nanoparticles (which were added at this concentration for mechanical reinforcement) in the PPF/PF-DA polymer was found to have no detrimental effect on bone ingrowth, bone contact, or degradability.

Acknowledgments

The authors are grateful for financial support from the National Institutes of Health (R01 AR48756) (A.G.M.) and Rice's Center for Biological and Environmental Nanotechnology through the National Science Foundation's Nanoscale Science and Engineering Initiative (EEC-0118007). The authors also thank Natasja van Dijk and Vincent Cuijpers for their assistance in this work.

REFERENCES

1. Mistry AS, Mikos AG. Tissue engineering strategies for bone regeneration. Adv Biochem Eng Biotechnol. 2005; 94:1–22. [PubMed: 15915866]
2. He S, Timmer MD, Yaszemski MJ, Yasko AW, Engel PS, Mikos AG. Synthesis of biodegradable poly(propylene fumarate) networks with poly(propylene fumarate)-diacrylate macromers as crosslinking agents and characterization of their degradation products. Polymer. 2000; 42(3):1251–1260.
3. Timmer MD, Ambrose CG, Mikos AG. In vitro degradation of polymeric networks of poly(propylene fumarate) and the crosslinking macromer poly(propylene fumarate)-diacrylate. Biomaterials. 2003; 24(4):571–577. [PubMed: 12437951]
4. Timmer MD, Ambrose CG, Mikos AG. Evaluation of thermal- and photo-crosslinked biodegradable poly(propylene fumarate)-based networks. J Biomed Mater Res, Part A. 2003; 66A(4):811–818.
5. Timmer MD, Horch RA, Ambrose CG, Mikos AG. Effect of physiological temperature on the mechanical properties and network structure of biodegradable poly(propylene fumarate)-based networks. J Biomater Sci Polym Ed. 2003; 14(4):369–382. [PubMed: 12747675]

6. Fisher JP, Vehof JW, Dean D, van der Waerden JP, Holland TA, Mikos AG, Jansen JA. Soft and hard tissue response to photocrosslinked poly(propylene fumarate) scaffolds in a rabbit model. J Biomed Mater Res. 2002; 59(3):547–556. [PubMed: 11774313]
7. Hedberg EL, Kroese-Deutman HC, Shih CK, Crowther RS, Carney DH, Mikos AG, Jansen JA. Effect of varied release kinetics of the osteogenic thrombin peptide TP508 from biodegradable, polymeric scaffolds on bone formation in vivo. J Biomed Mater Res, Part A. 2005; 72(4):343–353.
8. Horch RA, Shahid N, Mistry AS, Timmer MD, Mikos AG, Barron AR. Nanoreinforcement of poly(propylene fumarate)-based networks with surface modified alumoxane nanoparticles for bone tissue engineering. Biomacromolecules. 2004; 5(5):1990–1998. [PubMed: 15360315]
9. Mistry AS, Mikos AG, Jansen JA. Degradation and biocompatibility of a poly(propylene fumarate)-based/alumoxane nanocomposite for bone tissue engineering. J Biomed Mater Res A. 2007; 83A(4): 940–953. [PubMed: 17580323]
10. Mistry AS, Cheng SH, Yeh T, Christenson E, Jansen JA, Mikos AG. Fabrication and in vitro degradation of porous fumarate-based polymer/alumoxane nanocomposite scaffolds for bone tissue engineering. J Biomed Mater Res. Part A In press.
11. Shung AK, Timmer MD, Jo S, Engel PS, Mikos AG. Kinetics of poly(propylene fumarate) synthesis by step polymerization of diethyl fumarate and propylene glycol using zinc chloride as a catalyst. J Biomater Sci Polym Ed. 2002; 13(1):95–108. [PubMed: 12003078]
12. Mendenhall, HV. Animal Selection. In: Recum, AFv, editor. Handbook of Biomaterials Evaluation: Scientific, Technical, and Clinical Testing of Implant Materials. Philadelphia: Taylor and Francis; 1999. p. 475-479.
13. Bernhardt R, van den Dolder J, Bierbaum S, Beutner R, Scharnweber D, Jansen J, Beckmann F, Worch H. Osteoconductive modifications of Ti-implants in a goat defect model: characterization of bone growth with SR muCT and histology. Biomaterials. 2005; 26(16):3009–3019. [PubMed: 15603796]
14. Hedberg EL, Kroese-Deutman HC, Shih CK, Crowther RS, Carney DH, Mikos AG, Jansen JA. In vivo degradation of porous poly(propylene fumarate)/poly(DL-lactic-co-glycolic acid) composite scaffolds. Biomaterials. 2005; 26(22):4616–4623. [PubMed: 15722131]
15. Jansen JA, Dhert WJ, van der Waerden JP, von Recum AF. Semi-quantitative and qualitative histologic analysis method for the evaluation of implant biocompatibility. J Invest Surg. 1994; 7(2):123–134. [PubMed: 8049175]
16. De Jong WH, Eelco Bergsma J, Robinson JE, Bos RR. Tissue response to partially in vitro predegraded poly-L-lactide implants. Biomaterials. 2005; 26(14):1781–1791. [PubMed: 15576152]
17. Fisher JP, Holland TA, Dean D, Mikos AG. Photoinitiated cross-linking of the biodegradable polyester poly(propylene fumarate). Part II. In vitro degradation. Biomacromolecules. 2003; 4(5): 1335–1342. [PubMed: 12959603]
18. Hedberg EL, Shih CK, Lemoine JJ, Timmer MD, Liebschner MA, Jansen JA, Mikos AG. In vitro degradation of porous poly(propylene fumarate)/poly(DL-lactic-co-glycolic acid) composite scaffolds. Biomaterials. 2005; 26(16):3215–3225. [PubMed: 15603816]
19. Hedberg EL, Kroese-Deutman HC, Shih CK, Lemoine JJ, Liebschner MA, Miller MJ, Yasko AW, Crowther RS, Carney DH, Mikos AG. Methods: a comparative analysis of radiography, microcomputed tomography, and histology for bone tissue engineering. Tissue Eng. 2005; 11(9–10):1356–1367. [PubMed: 16259591]
20. Webster TJ, Ergun C, Doremus RH, Siegel RW, Bizios R. Enhanced functions of osteoblasts on nanophase ceramics. Biomaterials. 2000; 21(17):1803–1810. [PubMed: 10905463]
21. Lewandrowski KU, Bondre SP, Wise DL, Trantolo DJ. Enhanced bioactivity of a poly(propylene fumarate) bone graft substitute by augmentation with nano-hydroxyapatite. Biomed Mater Eng. 2003; 13(2):115–124. [PubMed: 12775902]
22. Ishaug SL, Crane GM, Miller MJ, Yasko AW, Yaszemski MJ, Mikos AG. Bone formation by three-dimensional stromal osteoblast culture in biodegradable polymer scaffolds. J Biomed Mater Res. 1997; 36(1):17–28. [PubMed: 9212385]

23. Ishaug-Riley SL, Crane-Kruger GM, Yaszemski MJ, Mikos AG. Three-dimensional culture of rat calvarial osteoblasts in porous biodegradable polymers. Biomaterials. 1998; 19(15):1405–1412. [PubMed: 9758040]

24. Burdick JA, Frankel D, Dernell WS, Anseth KS. An initial investigation of photocurable three-dimensional lactic acid based scaffolds in a critical-sized cranial defect. Biomaterials. 2003; 24(9): 1613–1620. [PubMed: 12559821]

25. Peter SJ, Lu L, Kim DJ, Mikos AG. Marrow stromal osteoblast function on a poly(propylene fumarate)/beta-tricalcium phosphate biodegradable orthopaedic composite. Biomaterials. 2000; 21(12):1207–1213. [PubMed: 10811302]

26. Vehof JW, Fisher JP, Dean D, van der Waerden JP, Spauwen PH, Mikos AG, Jansen JA. Bone formation in transforming growth factor beta-1-coated porous poly(propylene fumarate) scaffolds. J Biomed Mater Res. 2002; 60(2):241–251. [PubMed: 11857430]

Figure 1. Micro-CT analysis

A representative micro-CT reconstructed radiograph of a cross-section of a bone specimen with two implants within it. Bar is 5 mm.

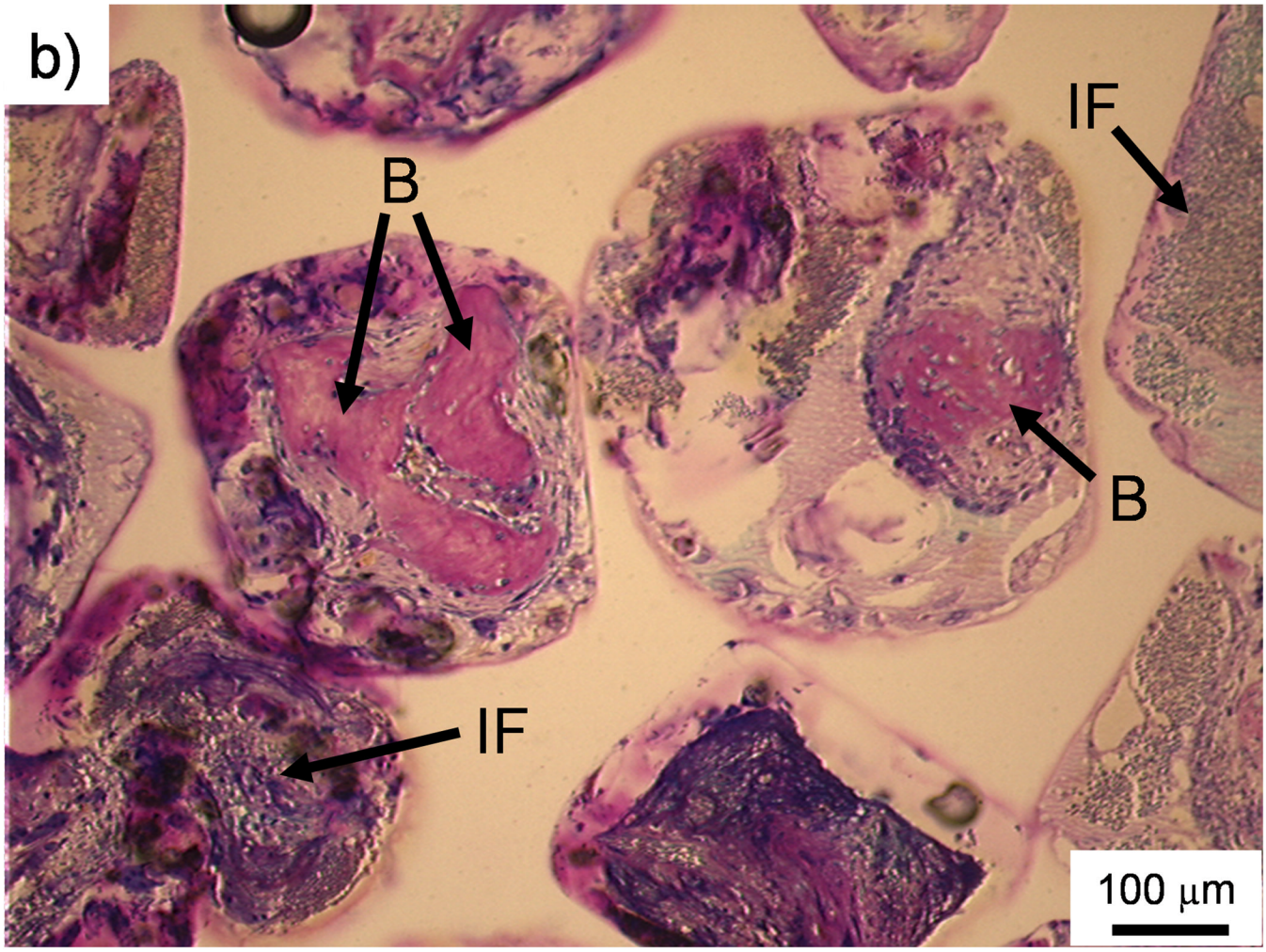

Figure 2. Histological sections: Bone formation and inflammation in pores

Histological sections from the top region of a PPF/PF-DA polymer alone sample. a) Round and pink tissue is immature bone, light pink tissue layers are fibrous tissue, and dark blue areas suggest inflamed tissue. Bar is 1 mm. b) Magnified image shows rounded pink areas of bone formation (B), dark blue areas of inflamed tissue and patches of small blue inflammatory cells (IF). Bar is 100 µm.

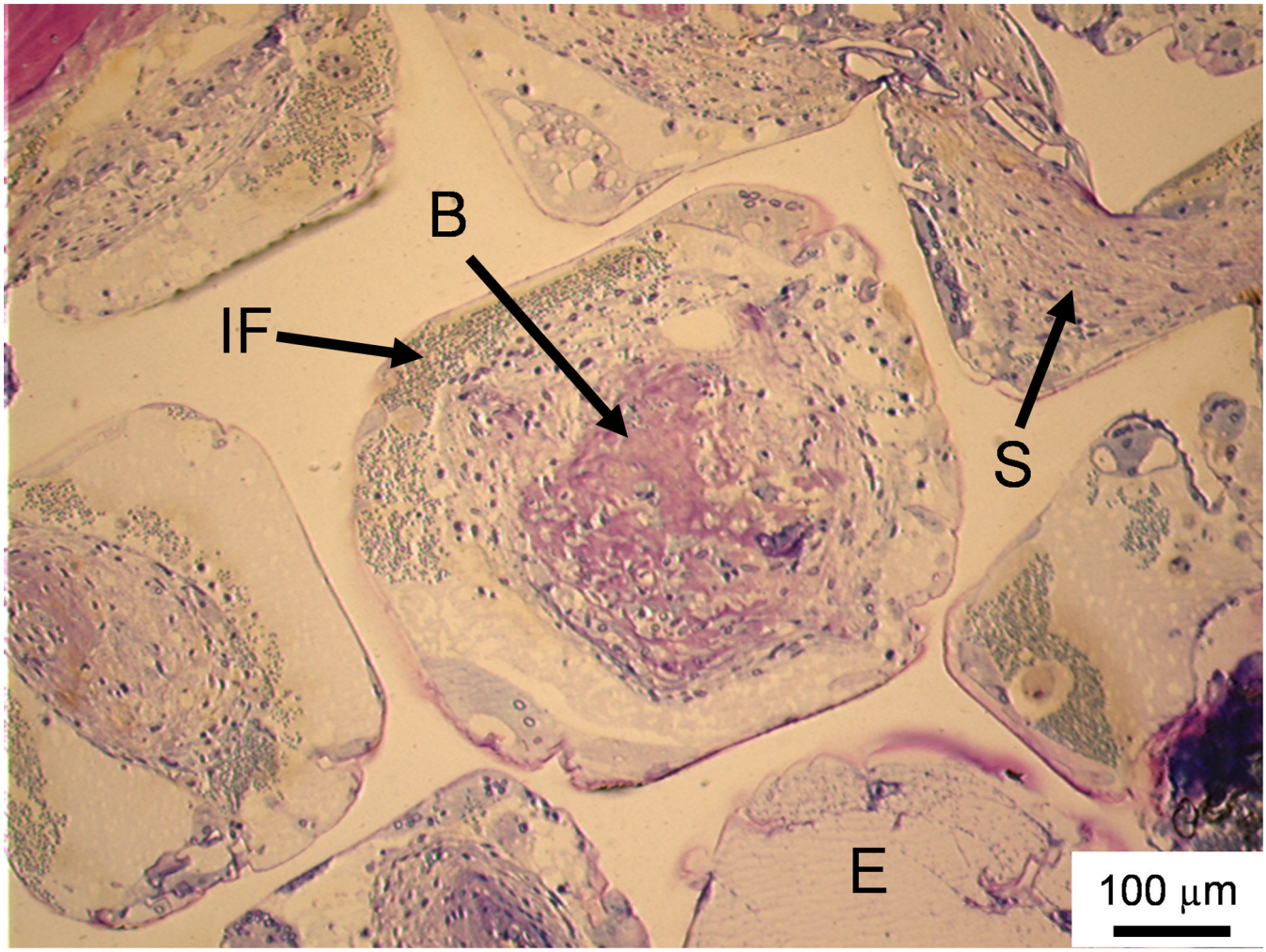

Figure 3. Histological sections: Soft tissue infiltration and bone formation in pores

Histological section from the middle region of a PPF/PF-DA polymer alone sample. Rounded pink tissue is immature bone (B), light pink tissue layers are fibrous tissue (S), and blue clusters of cells are inflammatory cells (IF). An empty or fluid filled pore is also visible (E). Bar is 100 µm.

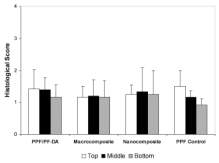

Figure 4. Histological scoring of bone growth within scaffold pores

Histological scoring of bone ingrowth for each material group based on Table 1. Data presented as mean ± standard deviation for $n = 3 – 6$. No statistically significant differences were observed between material groups or regions ($p > 0.05$).

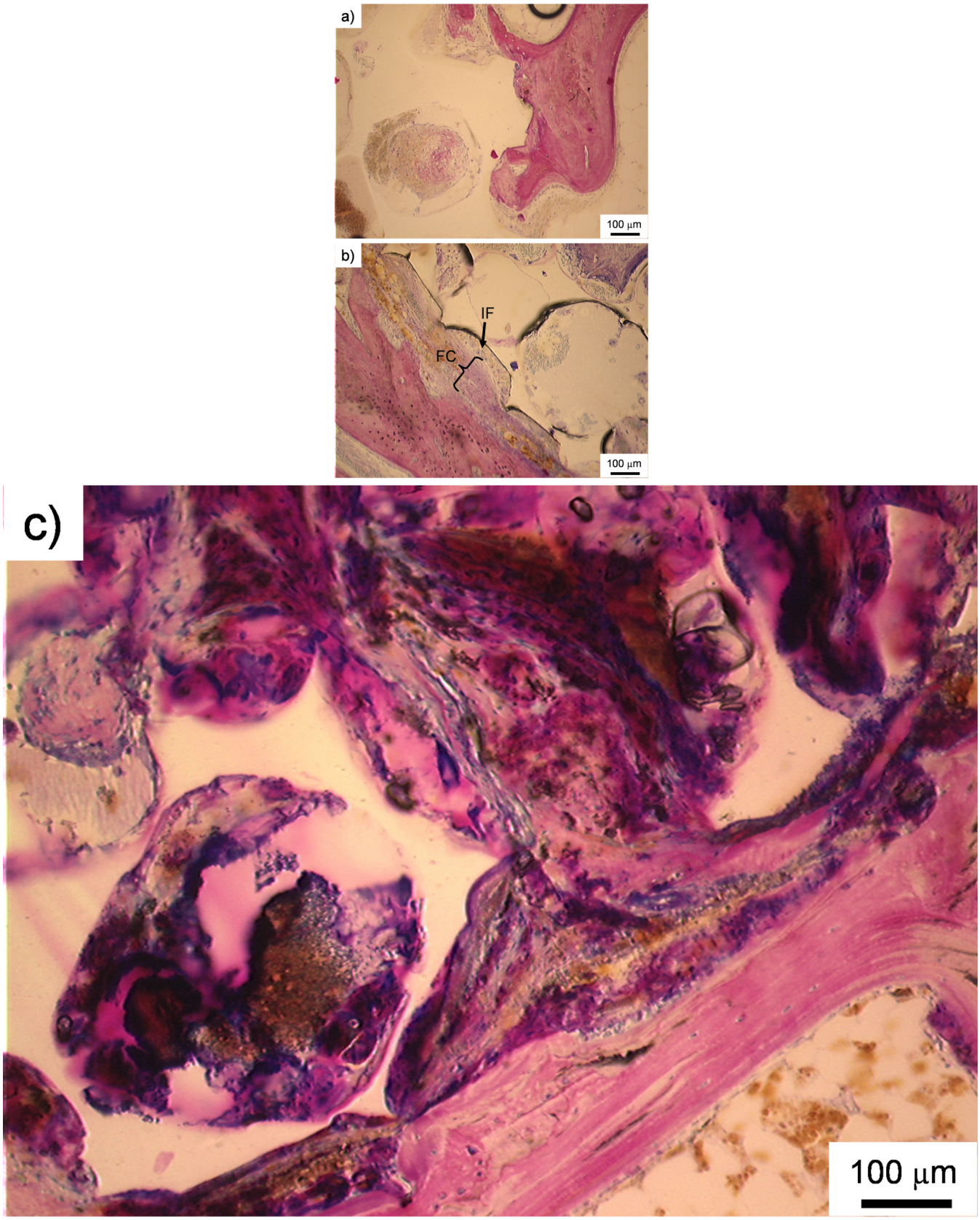

Figure 5. Histological sections

a) Histological section of the middle region of a PPF/PF-DA polymer alone scaffold. The white scaffold is in direct contact with the surrounding bone tissue (pink). Bar is 100 μm. b) Histological section of the top region of a macrocomposite scaffold showing a thin fibrous capsule (FC) surrounding the scaffold. The porous surface of the scaffold created a pocket where inflammatory cells (IF) accumulated. Bar is 100 μm. c) Histological section of the top region of a macrocomposite scaffold showing disorganized tissue and inflammatory cells at the scaffold-tissue interface. Bar is 100 μm.

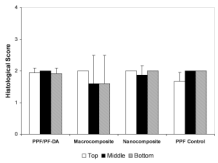

Figure 6. Histological scoring of bone contact at interface

Histological scoring of bone contact at the bone-scaffold interface for each material group based on Table 1. Data presented as mean ± standard deviation for $n = 3 – 6$. No statistically significant differences were observed between material groups or regions ($p > 0.05$).

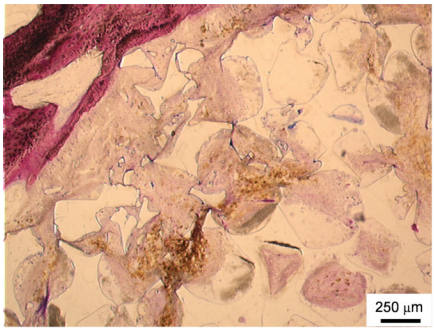

Figure 7. Histological section of *in vivo* degradation

Histological section from the top region of a PPF degradation control scaffold. Upper left area shows breakdown of polymer into smaller fragments and soft tissue infiltration with minimal inflammation. Bar is 250 μm.

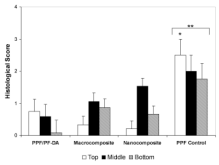

Figure 8. Histological scoring of degradation

Histological scoring of the *in vivo* degradation for each material group based on Table 1. Data presented as mean ± standard deviation for $n = 3 – 6$. The symbol "*" signifies a statistically significant difference compared to other materials within the same region ($p < 0.05$). The symbol "**" indicates a statistically significant difference of a material group compared with all other material groups with all region scores were combined ($p < 0.05$).

Table 1

Polymer and composite formulations

	Composition (wt.%)		
Material Group	**PPF**	**PF-DA**	**Particle**
PPF/PF-DA Polymer	33.33 %, M_n = 2740	66.67 %	0 %
PPF/PF-DA Macrocomposite	33.00 %, M_n = 2740	66.01 %	0.99 %, Boehmite microparticle
PPF/PF-DA Nanocomposite	33.00 %, M_n = 2740	66.01 %	0.99 %, Alumoxane nanoparticle
PPF Degradation Control	100 %, M_n = 750	0 %	0 %

Table 2

Histological scoring guides

Qualitative scoring guides used for histological scoring of each section based on the work of Hedberg et al. [7], Jansen et al. [15], and Mistry et al. [9]

Bone growth within scaffold pores

Description	Score
Tissue in pores is mostly bone	4
Tissue in pores consists of some bone with fibrous tissue and/or a few inflammatory response elements	3
Tissue in pores is mostly fibrous tissue (with or without bone) and young fibroblasts invading the space with few macrophages present	2
Tissue in pores consists mostly of inflammatory cells and connective tissue components in between (with or without bone) OR the majority of the pores are empty or filled with fluid	1
Tissue in pores is dense and exclusively of inflammatory type (no bone present)	0

Bone contact at interface

Description	Score
Direct bone to implant contact without soft tissue interlayer	4
Remodeling lacuna with osteoblasts and/or osteoclasts at surface	3
Majority of implant is surrounded by fibrous tissue capsule	2
Unorganized fibrous tissue (majority of tissue is not arranged as a capsule)	1
Inflammation marked by an abundance of inflammatory cells and poorly organized tissue	0

Polymer degradation

Description	Score
Abundant degradation – almost complete degradation or complete fragmentation	4
Marked degradation – several cracks in implant with presence of several fragments throughout implant	3
Moderate degradation – some cracks in implant and/or some fragments towards edges and outer surface	2
Minimal degradation – some minor dissolution on edges, minor cracks in implant and/or small fragments present	1
No degradation – Completely intact polymer	0

Table 3

Percentage bone volume

Percentage bone volume surrounding implanted scaffolds from each material group. Data presented as mean ± standard deviation for $n = 6$ for the PPF/PF-DA polymer alone and macrocomposite and n = 5 for the nanocomposite and low MW polymer group. No statistically significant differences were observed between material groups ($p > 0.05$).

Material Group	Bone Volume (%)
PPF/PF-DA Polymer	10.7 ± 4.5
PPF/PF-DA Macrocomposite	12.2 ± 3.5
PPF/PF-DA Nanocomposite	11.4 ± 2.9
PPF Degradation Control	11.9 ± 3.3

Table 4

Occurrence of bone in scaffold pores

The ratio of the occurrence of any amount of bone tissue within the pores of a sample to the total number of samples evaluated for each region and material group. The overall ratios for each material group and the percentage occurrence in sections are presented in the last two columns.

Material Group	Top	Middle	Bottom	Overall	In sections (%)
PPF/PF-DA Polymer	6/6	6/6	3/4	6/6	69.2
PPF/PF-DA Macrocomposite	2/4	5/5	4/5	6/6	65.0
PPF/PF-DA Nanocomposite	4/4	5/5	4/4	5/5	63.9
PPF Degradation Control	2/3	1/4	1/4	3/4	22.6
Total	14/17	17/20	12/17	20/21	57.9

Table 5

Occurrence of direct bone contact

The ratio of the occurrence of any amount of direct bone contact in a sample to the total number of samples evaluated for each region and material group. The overall ratios for each material group and the percentage occurrence in sections are presented in the last two columns.

Material Group	Top	Middle	Bottom	Overall	In sections (%)
PPF/PF-DA Polymer	5/6	5/6	2/4	5/6	40.4
PPF/PF-DA Macrocomposite	1/4	3/5	4/5	4/6	30.0
PPF/PF-DA Nanocomposite	1/4	2/5	3/4	2/5	30.6
PPF Degradation Control	3/3	3/4	3/4	4/4	58.1
Total	10/17	13/20	12/17	15/21	39.0